



## Partially coherent nonplanar sources

J C G deSande<sup>1</sup>, R Martínez-Herrero<sup>2</sup>, G Piquero<sup>2</sup>, O Korotkova<sup>3</sup>, M Santarsiero<sup>4</sup> and F Gori<sup>4</sup>

<sup>1</sup>*ETSISde Telecomunicación, Universidad Politécnica de Madrid Campus Sur, 28031 Madrid, Spain*

<sup>2</sup>*Departamentode Óptica, Universidad Complutense de Madrid*

*Ciudad Universitaria, 28040 Madrid, Spain*

<sup>3</sup>*Department of Physics, University of Miami*

*1320 Campo Sano Drive, Coral Gables, FL, 33146, USA*

<sup>4</sup>*Dipartimento di Ingegneria Industriale, Elettrotecnica e Meccanica, Università Roma Tre*

*ViaV. Volterra 62, 00146 Rome, Italy*

Dedicated to Professor Anna Consortini for her significant contributions and pioneering works in the field of atmospheric turbulence and her continuous commitment to promote optics at global level

Models for partially coherent spherical and cylindrical sources are presented, based on a decomposition into coherent modes of their cross-spectral densities. The primary coherence characteristics are computed both at the source surface and during propagation. Many examples with varying characteristics can be derived from the general expressions. Among others, an intriguing aspect of partially coherent spherical scalar sources is that, with a suitable choice of the weights of their component modes, the radiated field exhibits perfect radial coherence along any direction, while angular coherence is only partial. For the case of cylindrical symmetry, the study has been conducted for both scalar and vector sources. Interesting effects have been found concerning the evolution of the degree of coherence and the degree of polarization of the radiated field upon propagation. © Anita Publications. All rights reserved.

Doi: [10.54955/AJP.33.3-4.2024.185-196](https://doi.org/10.54955/AJP.33.3-4.2024.185-196)

Keywords: Nonplanar Sources; Coherence; Structured Light.

### 1 Introduction

Many studies focusing on partially coherent sources have predominantly explored planar sources [1-20]. However, it is worth noting that the Helmholtz equation offers analytical solutions with separable variables in a total of 11 coordinate systems [21]. Consequently, a wide range of non-planar sources can be considered. Interest in nonplanar sources has arisen from the advancements in optics within curved spaces [22-27]. Additionally, in the case of spherical sources, there is a notable connection to solar radiation [28,29]. Some studies have also been carried out on the propagation of cylindrical waves in nonlinear and inhomogeneous media, as well as the scattering of electromagnetic waves by cylinders [30-32].

In this context, we present recent significant findings related to two types of partially coherent nonplanar sources: those exhibiting spherical or cylindrical symmetry [33-36]. For the case of cylindrically symmetric sources, both scalar and vector treatment of the field is considered. For these two types of sources, we expand their cross-spectral density (CSD) at their surface using an incoherent superposition of coherent modes [1]. Subsequently, we obtain the corresponding CSD for the field propagating away from the source. We will unveil several features of the CSD through several illustrative examples.

Corresponding author

e mail: [massimo.santarsiero@uniroma3.it](mailto:massimo.santarsiero@uniroma3.it) (M Santarsiero)

The paper is structured as follows. This section constitutes the Introduction, and in the following section, some basic concepts will be recalled. Section (3) is devoted to the treatment of scalar spherical sources while in Section (4) both scalar and electromagnetic cylindrical sources will be studied. Finally, in Section 5 brief conclusions are resumed.

## 2 Preliminaries

The characteristics of a stationary scalar source can be appropriately studied through its CSD which can be expressed as

$$W(\mathbf{r}_1, \mathbf{r}_2) = \langle E^*(r_1)E(r_2) \rangle, \quad (1)$$

where  $E(\mathbf{r})$  is a scalar field and  $\mathbf{r}_j$  with  $j=1, 2$  are two points in the space outside the spherical or cylindrical source. Appropriate coordinates will be used for each case.

In particular, from the CSD, the spectral density and the degree of coherence can be obtained as [1]

$$I(\mathbf{r}) = W(\mathbf{r}, \mathbf{r}), \quad (2)$$

and

$$\mu(\mathbf{r}_1, \mathbf{r}_2) = \frac{W(\mathbf{r}_1, \mathbf{r}_2)}{\sqrt{W(\mathbf{r}_1, \mathbf{r}_1)W(\mathbf{r}_2, \mathbf{r}_2)}}, \quad (3)$$

respectively.

For the case of electromagnetic partially coherent sources, we make use of the  $3 \times 3$  cross-spectral density matrix (CSDM)  $\widehat{W}(\mathbf{r}_1, \mathbf{r}_2)$ , which accounts for the two-point second-order correlations between pairs of all field components, and whose elements are defined as [1,37,38]

$$W_{st}(\mathbf{r}_1, \mathbf{r}_2) = \langle E_s^*(\mathbf{r}_1)E_t(\mathbf{r}_2) \rangle \quad (s, t = r, \varphi, z) \quad (4)$$

the angle brackets denoting the ensemble average and cylindrical coordinates [ $r = (r, \varphi, z)$ ] have been used. The local characteristics of the field at the point  $\mathbf{r}$  are considered through the utilization of a matrix known as the polarization matrix

$$\widehat{P}(\mathbf{r}) = \widehat{W}(\mathbf{r}, \mathbf{r}) \quad (5)$$

Specifically, it allows for the determination of the spectral density of the field

$$S(\mathbf{r}) = \text{Tr}\{\widehat{P}(\mathbf{r})\}, \quad (6)$$

with  $\text{Tr}\{\cdot\}$  denoting the trace.

Various definitions of the degree of polarization (DOP) have been proposed for three-dimensional (3D) fields. One of these definitions, as presented in [39], is as follows

$$P_Q(r) = \sqrt{\frac{3}{2} \left[ \frac{\text{Tr}\{\widehat{P}^2(\mathbf{r})\}}{\text{Tr}^2\{\widehat{P}(\mathbf{r})\}} - \frac{1}{3} \right]} \quad (7)$$

This parameter is always limited to the interval (0, 1), the two limiting cases corresponding to completely unpolarized or perfectly polarized fields, respectively. It is worth noting that the following relation holds:

$$\frac{\text{Tr}\{\widehat{P}^2\}}{\text{Tr}^2\{\widehat{P}\}} = \frac{\lambda_1^2 + \lambda_2^2 + \lambda_3^2}{(\lambda_1 + \lambda_2 + \lambda_3)^2} \quad (8)$$

where  $\lambda_i$  ( $i = 1, 2, 3$ ) are the eigen values of  $\widehat{P}$ , so that  $P_Q$  can be expressed as

$$P_Q(r) = \frac{\sqrt{(\lambda_1 - \lambda_2)^2 + (\lambda_1 - \lambda_3)^2 + (\lambda_2 - \lambda_3)^2}}{\sqrt{2}(\lambda_1 + \lambda_2 + \lambda_3)} \quad (9)$$

A noteworthy point in this definition is that for a completely unpolarized 2D field, the DOP is 1/2. In this scenario, one of the eigen values is zero, while the other two are equal, indicating the presence of a certain level of "polarization". This occurs because one of the three field components is absent.

Alternative definitions for a 3D DOP have been given. For example, Ellis *et al* [40] introduced the following parameter, which reduces to the usual one for 2D field:

$$P_L(r) = \frac{\lambda_1 - \lambda_2}{(\lambda_1 + \lambda_2 + \lambda_3)}, \quad (10)$$

with the eigen values ordered in such a way that  $\lambda_1 \geq \lambda_2 \geq \lambda_3$ . In fact, if the field is 2D, then  $\lambda_3 = 0$ , and  $P_L$  gives 0 for completely unpolarized fields ( $\lambda_1 = \lambda_2$ ) and 1 for completely polarized fields ( $\lambda_2 = 0$ ). Comparisons and relationships between the above definitions can be found in [41-43].

On the other hand, several scalar quantities have been suggested to describe the coherence characteristics of the field in the literature [37,44-49]. However, most of these measures pertain to paraxial fields, where the longitudinal field component can be disregarded, resulting in the reduction of the cross-spectral density (CSD) matrix to a 2×2 matrix. In the most general context, an electromagnetic degree of coherence can be introduced as proposed by Setälä [37].

$$\mu_Q(\mathbf{r}_1, \mathbf{r}_2) = \frac{\sqrt{\text{Tr}\{\widehat{W}^\dagger(\mathbf{r}_1, \mathbf{r}_2)\widehat{W}(\mathbf{r}_1, \mathbf{r}_2)\}}}{\sqrt{S(\mathbf{r}_1)S(\mathbf{r}_2)}}, \quad (11)$$

the dagger denoting the adjoint. Since the following relation holds:

$$\text{Tr}\{\widehat{W}^\dagger(\mathbf{r}_1, \mathbf{r}_2)\widehat{W}(\mathbf{r}_1, \mathbf{r}_2)\} = \sum_{st} |W_{st}(\mathbf{r}_1, \mathbf{r}_2)|^2 \quad (s, t = r, \varphi, z), \quad (12)$$

the function  $\mu_Q(\mathbf{r}_1, \mathbf{r}_2)$  accounts for all correlations among the field components equally. However, in accordance with this definition, the relation  $\mu_Q(\mathbf{r}_1, \mathbf{r}_2) = 1$  does not generally hold, unlike in the scalar case, as non-perfect correlations may exist among various field components at a single point. This is particularly the case when the field is not perfectly polarized. In fact, it can be proved that

$$\mu_Q(\mathbf{r}, \mathbf{r}) = \sqrt{\frac{2P_Q(\mathbf{r}) + 1}{3}}, \quad (13)$$

**indicating that  $\mu_Q(\mathbf{r}, \mathbf{r}) = 1$  is only valid for perfectly polarized fields.**

Another definition for the degree of coherence in three-dimensional fields was introduced in Ref [45]:

$$\mu_L(\mathbf{r}_1, \mathbf{r}_2) = \frac{\text{Tr}\{\widehat{W}(\mathbf{r}_1, \mathbf{r}_2)\}}{\sqrt{S(\mathbf{r}_1)S(\mathbf{r}_2)}} \quad (14)$$

This definition is consistent in form with classic coherence theory, as it involves the norm of the linear CSDM. It preserves phase information, making it crucial for applications such as remote directional control and singular optics.

### 3 Spherical sources

Within this section, a generic point will be expressed in spherical coordinates,  $\mathbf{r} = (r, \vartheta, \varphi)$ , where  $r$ ,  $\vartheta$  and  $\varphi$  denote the distance to the origin, the polar and the azimuthal angle, respectively. The CSD of a scalar partially coherent spherical source can be expressed as a modal expansion of the form

$$W_s(\vartheta_1, \varphi_1; \vartheta_2, \varphi_2) = \sum_{l=0}^{\infty} \sum_{m=-l}^l A_{lm} Y_l^{m*}(\vartheta_1, \varphi_1) Y_l^m(\vartheta_2, \varphi_2), \quad (15)$$

where  $A_{lm}$  are non-negative coefficients. The asterisk indicates complex conjugate and the symbol  $Y_l^m(\vartheta, \varphi)$  specifies the spherical harmonic of indexes  $l$  and  $m$ , defined as in [50]:

$$Y_l^m(\vartheta, \varphi) = \sqrt{\frac{2l+1}{4\pi} \frac{(l-m)!}{(l+m)!}} P_l^m(\cos \vartheta) e^{im\varphi}, \quad (l = 0, 1, \dots; m = 0, \pm 1, \pm 2, \dots \pm l), \quad (16)$$

being  $P_l^m$  the Legendre function of orders  $l$  and  $m$  [50].

The spherical harmonics enable us to express a solution to the propagation problem for all points in space outside the source as a modal expansion using well-known functions. In fact, each of the functions  $P_l^m(\cos \vartheta)$ ,  $\exp(im\varphi)$  as seen in Eq (16) can be combined with a radial component to form a solution to the wave equation. To achieve this, we employ the outgoing spherical Hankel functions [51], denoted as  $H_l(kr)$ , where  $k$  represents the wavenumber. If the radial part is selected as  $H_l(kr)/H_l(ka)$ , with  $a$  being the radius of the spherical source, the solution satisfies the boundary condition by assuming prescribed values at the source's surface.

By employing Eqs (15) and (16) and incorporating the radial components, expressed in terms of the outgoing Hankel function [50],  $H_l$ , the CSD takes the form [52]:

$$W(r_1, r_2; \vartheta_1, \vartheta_2; \varphi_1, \varphi_2) = \sum_{l=0}^{\infty} \sum_{m=-l}^l c_{lm} e^{im(\varphi_2 - \varphi_1)} P_l^m(\cos \vartheta_1) P_l^m(\cos \vartheta_2) \frac{H_l^*(kr_1) H_l(kr_2)}{|H_l(ka)|^2}, \quad (17)$$

In this equation, the coefficients  $c_{lm}$  are non-negative, with  $l$  ranging from 0 onwards and  $m$  from  $-l$  to  $l$ . Notably, the dependence of  $W$  on  $r_1$  and  $r_2$  occurs through the functions  $H_l$ , which are solely dependent on the index  $l$ . The latter can be considered as specifying the  $l$ -th radial mode of the CSD. For each radial mode, there are  $2l+1$  angular structures, each of them being determined by the index  $m$ . These functions, which are proportional to the spherical harmonics will be referred to as the angular modes.

From the CSD, the spectral density can be obtained as

$$S(r, \vartheta) = \sum_{l=0}^{\infty} \sum_{m=-l}^l c_{lm} \left| P_l^m(\cos \vartheta) \frac{H_l(kr)}{H_l(ka)} \right|^2, \quad (18)$$

An interesting implication that follows from Eq (18) is that the spectral density on the surface of any sphere concentric with the source is independent of the azimuthal angle but generally varies with polar angle. A straight forward example that supports this observation is depicted in Fig 1(a), where the spectral density has been calculated on the source surface and only two terms of the modal expansion are considered. The spectral density remains constant at any latitude and is symmetric with respect to the equator, which is characteristic of spherical sources with harmonic modes [33].

The degree of coherence can be obtained by substituting the expression of the CSD of Eq (17) into the Eq (3). Even for this simple case the degree of coherence relative to a given point, the absolute value of the degree of coherence remains constant along the polar coordinate  $\vartheta$  (see Fig 1(b)). In this particular example, with  $m = \pm 2$ , the degree of coherence relative to a specific point displays a periodicity of  $\pi$  along the azimuthal coordinate, as illustrated in, Fig 1(b) and (c). A pair of coherency vortices is seen to appear in correspondence of the poles.

Closed-form expressions have been obtained for various selections of the coefficients  $c_{lm}$  [33], and by adjusting these weights, a wide range of behaviors can be observed for spectral density and for the degree of coherence.

As a first example, we show that a category of CSDs exists that exhibit no dependence on the azimuthal angles,  $\varphi_1$  and  $\varphi_2$ . This scenario arises when all the coefficients in Eq (17) become zero except for those with  $m = 0$ . Since all the  $c_{l0}$  coefficients are non-negative and the squared Legendre polynomials

reach their maximum at  $\vartheta = 0$  and  $\pi$ , the intensity will peak at the poles regardless of the specific values of the  $c_{l0}$  coefficients. Conversely, the equatorial region will be dim, and complete darkness will be observed at the equator if the coefficients  $c_{l0}$  are zero for all even  $l$  indices [33]. This class of sources exhibits complete coherence for all points located on the same latitude. Beyond that latitude, it gradually becomes more incoherent as the number of considered modes increases. Additionally, at a latitude symmetrical to the equator, the source remains fully coherent, that is  $|\mu(\vartheta_1 = \vartheta_2)| = |\mu(\vartheta_1 = \pi - \vartheta_2)| = 1$ .

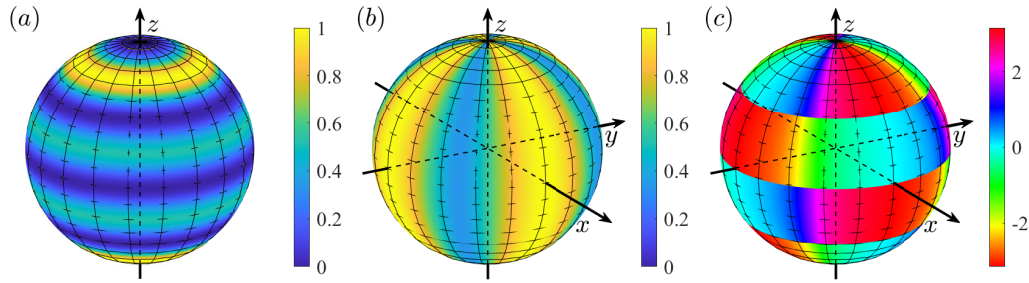


**Fig 1.** (a) The spectral density on the surface of a spherical source, as described by Eq (18), with all coefficients being  $c_{lm} = 0$ , except for  $c_{5,2} = 1$  and  $c_{5,-2} = 0.5$ . (b) The absolute value and (c) the phase of the corresponding degree of coherence when  $\varphi_2 = 0$  and  $\vartheta_2 = \pi/2$ .

Another interesting case appears when only modes with  $m = l$  enter the expansion given by Eq (17). Then the following relation can be used [51]

$$Y_l^l(\vartheta, \varphi) \propto \sin^l \vartheta e^{il\varphi}, \quad (l = 0, 1, \dots), \quad (19)$$

where a proportionality factor have been omitted. In this case, the spectral density reaches its maximum near the equator, and the degree of coherence presents complex structures [33].

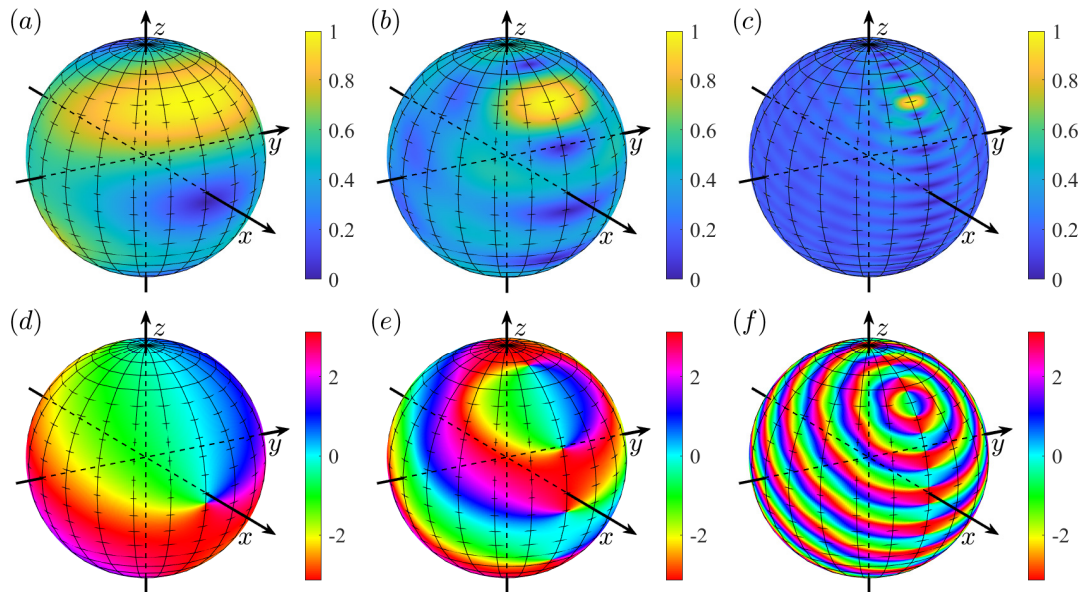


**Fig 2.** Absolute value (a-c) and phase (e-f) of the degree of coherence as a function of a point on the source surface when the other one has coordinates  $\varphi_2 = 0$  and  $\vartheta_2 = \pi/2$ . Only the terms with  $l = l_0$  are present in the sum:  $l_0 = 2$  (a, d);  $l_0 = 5$  (b, e);  $l_0 = 20$  (c, f).

A third interesting situation arises when only one value of index  $l$  is considered in Eq (17). In this case, there is a contribution of  $2l + 1$  angular modes that share the same radial dependence. Consequently, it is possible to achieve perfect radial coherence while allowing for a decrease in angular coherence as the number of angular modes increases. To illustrate this concept, Fig 2 shows the absolute value of the degree of coherence for the source defined by Eq (17), where  $c_{lm} = f_m \delta_{l, l_0}$  and  $\delta_{nm}$  is the Kronecker delta. The coefficients  $f_m$  are chosen in such a way that all the angular modes involved carry the same energy. It can be noted that for lower values of  $l_0$ , two extensive regions exist with high coherence (see Fig 2(a)). However, as the value of  $l_0$  increases, these two regions become smaller and smaller, and the coherence outside these regions decreases to a negligible level (see Fig 2(b) and (c)). On the other hand, the phase shows an increasing number of vortices (see Fig 2(d)-(f)). Similar results are obtained for arbitrary choices of  $f_m$  (even when they are randomly chosen [33]).

#### 4 Cylindrical sources

In this section, we will represent a generic point in cylindrical coordinates as  $\mathbf{r} = (r, \varphi, z)$ , where  $r$  is the radial distance to the  $z$ -axis,  $\varphi$  is the azimuthal angle, and  $z$  is the axial coordinate or height. Let us examine a cylinder with radius  $a$  that extends infinitely along the  $z$ -axis (refer to Fig 3). Thanks to its cylindrical symmetry, we assume that the emitted field remains independent of the  $z$  coordinate. Consequently, the electric field in the external space can be expressed as a function solely of  $r$  and  $\varphi$ . This scenario requires a vectorial treatment and polarization effects must be taken into account.

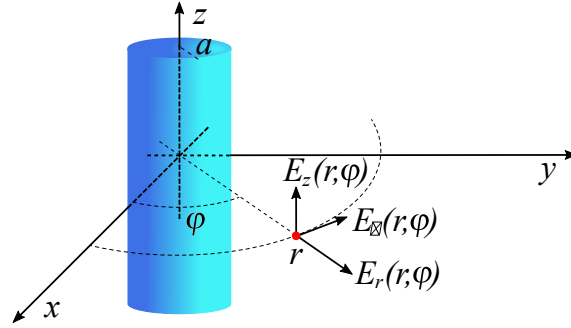


Fig 3. Section of an infinitely long cylinder of radius  $a$  showing the generated electric field components at an arbitrary point  $(r, \varphi)$ .

In this geometric configuration, three possibilities can be considered (see Fig 3): the electric field is parallel to the  $z$ -axis ( $E$  polarization); the magnetic field is parallel to the  $z$ -axis ( $H$  polarization), leading to an electric field vector with radial and azimuthal components perpendicular to the  $z$ -axis; both the above polarizations are present simultaneously.

Let us start with the simplest case of  $E$  polarization. According to [50,53] the outgoing irradiated field can be expanded into the series

$$E_z(r, \varphi) = \sum_{n=-\infty}^{\infty} b_n H_n(kr) e^{in\varphi} \hat{z}; \quad (r \geq a), \quad (20)$$

with a suitable set of  $b_n$  coefficients. This  $z$ -component of the field can be written as

$$E_z(r, \varphi) = \sum_{n=-\infty}^{\infty} c_n Z_n(kr) e^{in\varphi}; \quad (r \geq a), \quad (21)$$

where

$$c_n = b_n H_n(ka); \quad Z_n(K_r) = \frac{H_n(kr)}{H_n(ka)}. \quad (22)$$

The  $c_n$  coefficients correspond to the standard Fourier coefficients of  $E_z$  along a circle with a radius of  $r = a$ , because for all  $n$ ,  $Z_n(ka) = 1$ .

Similar expansion can be used in  $H$  polarization to express the magnetic induction  $\mathbf{B}$  along the  $z$ -axis, namely,

$$\mathbf{B}_z(r, \varphi) = \sum_{n=-\infty}^{\infty} d_n Z_n(kr) e^{in\varphi} \hat{z} \quad (r \geq a), \quad (23)$$

with a different set of coefficients  $\{d_n\}$ .

If the field propagates in vacuum, the corresponding electric field can be evaluated as [50,51]

$$\mathbf{E}_t(\mathbf{r}) = \frac{ic}{k} \nabla \times \mathbf{B}_z(\mathbf{r}) \quad (24)$$

with  $c$  being the speed of light. This results in two transverse components

$$\begin{cases} \mathbf{E}_r(r, \varphi) = \frac{ic}{kr} \frac{\partial B_z}{\partial \varphi} = -c \sum_{n=-\infty}^{\infty} n d_n \frac{Z_n(kr)}{kr} e^{in\varphi}, \\ \mathbf{E}_\varphi(r, \varphi) = -\frac{ic}{kr} \frac{\partial B_z}{\partial r} = -ic \sum_{n=-\infty}^{\infty} d_n Z'_n(kr) e^{in\varphi}, \end{cases} \quad (25)$$

the prime denoting derivative with respect to the argument.

As for the case of  $E$ -polarization, we can set

$$a_n = -ic d_n, \quad (26)$$

and

$$R_n(kr) = \frac{-in}{H_n(ka)} \frac{H_n(kr)}{kr} \quad (27)$$

Taking into account the contributions of the two polarizations, as illustrated in Fig 3, we can formulate the following expressions for the three components (namely, radial, tangential, and axial) of the electric field throughout space:

$$\begin{cases} \mathbf{E}_r(r, \varphi) = \sum_{n=-\infty}^{\infty} a_n R_n(kr) e^{in\varphi}, \\ \mathbf{E}_\varphi(r, \varphi) = \sum_{n=-\infty}^{\infty} a_n \Phi_n(kr) e^{in\varphi}, \\ \mathbf{E}_z(r, \varphi) = \sum_{n=-\infty}^{\infty} c_n Z_n(kr) e^{in\varphi}. \end{cases} \quad (28)$$

In the following, the functions  $R_n$ ,  $\Phi_n$ , and  $Z_n$  will be referred to as the radial, tangential, and axial basis functions of the field, respectively.

The behavior of these functions in propagation has been thoroughly examined in prior studies [33-36]. A low-pass filtering effect concerning the index  $n$  has been observed [33,34]: as the index  $n$  exceeds the value of  $ka$ , the corresponding basis function exhibits a progressively sharper decrease in the proximity of the cylinder surface. This implies that while basis functions with various index values contribute to the field near the source surface, only those with low index values remain significant at a short distance from the cylinder surface.

Conversely, the absolute values of the tangential and axial basis functions decrease with  $r^{-1/2}$  when  $kr \gg n$ , while the radial component decreases as  $r^{-3/2}$ , rendering it less and less significant after a certain propagation distance (several times the cylinder radius). This indicates that at a considerable distance from the cylinder surface, the electric field is essentially orthogonal to the radial direction [35,36].

A partially coherent field is achieved when the coefficients  $a_n$  and  $c_n$  become random variables. The following are the explicit expressions of the nine elements of the CSD matrix in Eq (4), for the most general case:

$$\begin{aligned}
W_{rr}(r_1, r_2) &= \sum_{n, m} \langle a_n^* a_m \rangle R_n^*(kr_1) R_m(kr_2) e^{-in\varphi_1 + im\varphi_2} \\
W_{\varphi\varphi}(r_1, r_2) &= \sum_{n, m} \langle a_n^* a_m \rangle \Phi_n^*(kr_1) \Phi_m(kr_2) e^{-in\varphi_1 + im\varphi_2} \\
W_{zz}(r_1, r_2) &= \sum_{n, m} \langle c_n^* c_m \rangle Z_n^*(kr_1) Z_m(kr_2) e^{-in\varphi_1 + im\varphi_2} \\
W_{r\varphi}(r_1, r_2) &= \sum_{n, m} \langle a_n^* a_m \rangle R_n^*(kr_1) \Phi_m(kr_2) e^{-in\varphi_1 + im\varphi_2} \\
W_{rz}(r_1, r_2) &= \sum_{n, m} \langle a_n^* c_m \rangle R_n^*(kr_1) Z_m(kr_2) e^{-in\varphi_1 + im\varphi_2} \\
W_{\varphi z}(r_1, r_2) &= \sum_{n, m} \langle a_n^* c_m \rangle \Phi_n^*(kr_1) Z_m(kr_2) e^{-in\varphi_1 + im\varphi_2}. \\
W_{\varphi r}(r_1, r_2) &= W_{r\varphi}^*(r_2, r_1), \quad W_{zr}(r_1, r_2) = W_{rz}^*(r_2, r_1), \quad W_{z\varphi}(r_1, r_2) = W_{\varphi z}^*(r_2, r_1)
\end{aligned} \tag{29}$$

Depending on the choice of correlations  $\langle a_n^* a_m \rangle$ ,  $\langle c_n^* c_m \rangle$  and  $\langle c_n^* a_m \rangle$ , a wide variety of behaviors can be found.

A first interesting choice is  $a_n = 0$  for any  $n$ , so that  $\langle a_n^* a_m \rangle = \langle c_n^* a_m \rangle = 0$ ,  $\forall (n, m)$ , in which case only the axial component of the field remains (see Fig 3). This case can be treated as a scalar source [34] which is totally polarized (PQ = PL = 1) everywhere [35,36]. Some interesting results have been found for this family of sources. For example, when all the modes are considered perfectly uncorrelated ( $\langle c_n^* c_m \rangle = \gamma_n \delta_{nm}$ , being  $\delta_{nm}$  the Kronecker delta), the CSD becomes angularly homogeneous, that is, it depends on the angular shift  $\Delta\varphi = \varphi_2 - \varphi_1$ . Moreover, if  $\langle c_n^* c_m \rangle = A$  for  $|n| \leq N$  and  $\langle c_n^* c_m \rangle = 0$  otherwise, the degree of coherence nearly follows a sinc behavior on the cylinder surface and approaches a besinc behavior as the propagation distance increases [34]. A low-pass filtering effect is also observed in propagation. Although modes of any order contribute to the CSD on the cylinder surface, only those modes with order upto  $ka$  significantly contribute to the spectral density and to the degree of coherence after a given propagation distance [34].

A second interesting possibility is  $c_n = 0$  for any  $n$  (so that  $\langle c_n^* c_m \rangle = \langle c_n^* a_m \rangle = 0$ ,  $\forall (n, m)$ ), in which case the axial component vanishes (see Fig 3) and the electric field lies in a plane perpendicular to the cylinder axis. This field is, in general, partially polarized and its degree of polarization evolves during propagation in a way depending on the choice of  $\langle a_n^* a_m \rangle$ . For example, if  $\langle a_n^* a_m \rangle = An^2 \delta_{nm}$  for  $|n| \leq N$  and  $\langle a_n^* a_m \rangle = 0$  otherwise, the degree of coherence reaches a minimum value in propagation if the number of modes is close to or over  $2ka$ . This minimum value is 0.5 if the degree of polarization is calculated as Eq (7) or zero if it is calculated according to Eq (10). Note that in this case, the electric field is a 2D field (the axial component vanishes), so according to the definition in Eq (7), this field is still partially polarized.

A more general class of cylindrical partially coherent sources arises when all the involved expansion coefficients are mutually uncorrelated, that is, when in Eq (29) we take,

$$\langle a_n^* a_m \rangle = \alpha_n \delta_{nm}, \quad \langle c_n^* c_m \rangle = \gamma_n \delta_{nm} \quad \text{and} \quad \langle c_n^* a_m \rangle = 0, \tag{30}$$

where  $\alpha_n$  and  $\gamma_n$  are positive quantities and  $\delta_{nm}$  is the Kronecker delta. This choice corresponds to considering the partially coherent field as the result of incoherent superposition of perfectly coherent and perfectly polarized vector modes [54,55]. In this case, CSD matrix becomes angularly homogeneous, that is, it depends only on the angular difference,  $\Delta\varphi = \varphi_2 - \varphi_1$  [35,36] and then, the polarization matrix and the spectral density are independent of the azimuthal angle. The evolution of the spectral density as well as the polarization properties with the propagation distance have been studied through several examples in [35,36].



A simple class of angularly inhomogeneous CSDM's is obtained if the correlations are chosen as

$$\langle a_n^* a_m \rangle = \alpha_n (\delta_{nm} + \delta_{n,-m}); \langle c_n^* c_m \rangle = \gamma_n (\delta_{nm} + \delta_{n,-m}); \langle c_n^* a_m \rangle = \beta_n (\delta_{nm} + \delta_{n,-m}), \quad (31)$$

with  $\alpha_0 = \gamma_0 = \beta_0$ . In this case the CSDM results

$$\widehat{W}(\mathbf{r}_1, \mathbf{r}_2) = \sum_{n=1}^{\infty} \widehat{W}_n(r_1, r_2) \cos(n\varphi_1) \cos(n\varphi_2) \quad (32)$$

where

$$\widehat{W}(\mathbf{r}_1, \mathbf{r}_2) = \begin{pmatrix} a_n R_n^*(kr_1) R_n(kr_2) & a_n R_n^*(kr_1) \Phi_n(kr_2) & \beta_n R_n^*(kr_1) Z_n(kr_2) \\ a_n \Phi_n^*(kr_1) R_n(kr_2) & a_n \Phi_n^*(kr_1) \Phi_n(kr_2) & \beta_n \Phi_n^*(kr_1) Z_n(kr_2) \\ \beta_n Z_n^*(kr_1) R_n(kr_2) & \beta_n Z_n^*(kr_1) \Phi_n(kr_2) & \gamma_n Z_n^*(kr_1) Z_n(kr_2) \end{pmatrix} \quad (33)$$

Figure 4 shows the spectral density (a-d) and the 3D-degree of polarization (e-f) in the region  $a < r < 5a$ , for a source with a CSDM as in Eq (32) with  $ka = 100$  and the coefficients such that  $\beta_n = 0$  and  $\alpha_n = n, \gamma_n = n^2$  for  $n \leq N$  and  $\alpha_n = \gamma_n = 0$  otherwise. Plots refer to different values of  $N$ :  $N = 3$  (a, e);  $N = 5$  (b-f);  $N = 10$  (c, g);  $N = 15$  (d, h). The behavior of the spectral density reveals the presence of  $2N$  radiation lobes, two of which carry higher power, while the polarization degree presents angular dependence and increases with increasing the number of modes. Such behaviors, however, can be significantly varied by acting on the correlation coefficients.

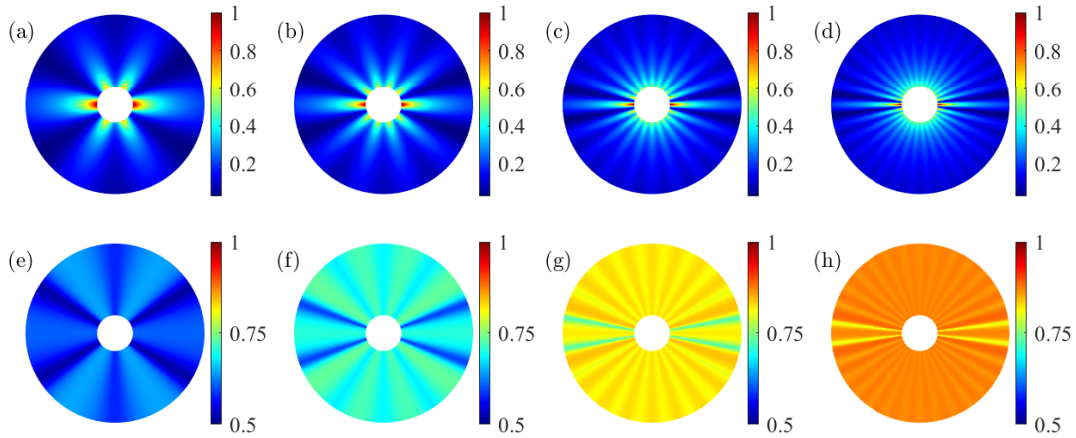


Fig 4. Spectral density (a-d) and 3D-degree of polarization  $P_Q$  (e-h) in the region,  $a < r < 5a$ , for a source with CSDM given in Eq (32) with  $k_a = 100$  and the following coefficients:  $\beta_n = 0$  and  $\alpha_n = n, \gamma_n = n^2$  for  $n \leq N$ , and  $\alpha_n = \gamma_n = 0$  for  $n > N$ . Plots refer to different values of  $N$ :  $N = 3$  (a,e);  $N = 5$  (b-f);  $N = 10$  (c,g);  $N = 15$  (d,h).

## 5 Conclusions

Two classes of partially coherent nonplanar sources have been introduced. The first one is defined on a spherical surface, and the CSDs of the sources belonging to this class can be obtained by superimposing spherical harmonic functions with non negative weights. In some cases, depending on the choice of the weights, the resulting CSD takes a simple analytical form. By considering the propagation of each spherical harmonic function the expression of the propagated CSD can be evaluated in a straight forward way. In particular, this approach enables the analysis of the radial coherence features of the propagated field. It is worth noting that when the mode superposition is limited to spherical harmonic functions with the same  $l$  value, the radiated field exhibits perfect radial coherence during propagation, while its angular coherence is only partial.

The second class includes partially coherent electromagnetic sources across the surface of a cylinder. Due to the different behaviors of the three components of the electric field across the source and during propagation, the spectral density and the degree of polarization may present very diverse features. A quite general class of cylindrical sources has been found that can be described as an incoherent superposition of coherent vector modes, expressed in terms of Hankel functions. By manipulating the mode coupling coefficients, it becomes possible to control spectral density, coherence, and polarization characteristics of the radiated field, for any polarization state of the source. Such a possibility makes the presented models interesting for applications in several applications, such as directional illumination and sensing.

## References

1. Mandel L, Wolf E, *Optical Coherence and Quantum Optics*, (Cambridge University Press), 1995.
2. Korotkova O, *Theoretical Statistical Optics*, (Hackensack N J, World Scientific), 2021.
3. James D F V, Change of polarization of light beams on propagation in free space, *J Opt Soc Am A*, 11(1994)1641–1643.
4. Gori F, Santarsiero M, Vicalvi S, Borghi R, Guattari G, Beam coherence-polarization matrix, *Pure Appl Opt*, 7(1998)941–951.
5. Tervo J, Azimuthal polarization and partial coherence, *J Opt Soc Am A*, 20(2003)1974–1980.
6. Ramírez-Sánchez V, Piquero G, Santarsiero M, Synthesis and characterization of partially coherent beams with propagation-invariant transverse polarization pattern, *Opt Commun*, 283(2010)4484–4489.
7. Santarsiero M, Ramírez-Sánchez V, Borghi R, Partially correlated thin annular sources: the vectorial case, *J Opt Soc Am A*, 27(2010)1450–1456.
8. Guo L, Tang Z, Liang C, Tan Z, Intensity and spatial correlation properties of tightly focused partially coherent radially polarized vortex beams, *Opt Laser Technol*, 43(2011)895–898.
9. de Sande J C G, Santarsiero M, Piquero G, Gori F, Longitudinal polarization periodicity of unpolarized light passing through a double wedge depolarizer, *Opt Express*, 20(2012)27348–27360.
10. Santarsiero M, de Sande J C G, Piquero G, Gori F, Coherence–polarization properties of fields radiated from transversely periodic electromagnetic sources, *J Opt*, 15(2013)055701; doi.10.1088/2040-8978/15/5/055701.
11. Chen Y, Wang F, Liu L, Zhao C, Cai Y, Korotkova O, Generation and propagation of a partially coherent vector beam with special correlation functions, *Phys Rev A*, 89(2014)013801; doi.org/10.1103/PhysRevA.89.013801.
12. Mei Z, Korotkova O, Electromagnetic Schell-model sources generating far fields with stable and flexible concentric rings profiles, *Opt Express*, 24(2016)5572–5583.
13. Xu H.-F, Zhou Y, Wu H.-W, Chen H.-J, Sheng Z.-Q, Qu J, Focus shaping of the radially polarized Laguerre-Gaussian-correlated Schell-model vortex beams, *Opt Express*, 26(2018)20076–20088.
14. Senthilkumar M, Rajesh K, Udhayakumar M, Jaroszewicz Z, Mahadevan G, Focusing properties of spirally polarized sinh Gaussian beam, *Opt Laser Technol*, 111(2019)623–628.
15. Hyde M W, Xiao X, Voelz D G, Generating electromagnetic nonuniformly correlated beams, *Opt Lett*, 44(2019)5719–5722.
16. Yu J, Zhu X, Lin S, Wang F, Gbur G, Cai Y, Vector partially coherent beams with prescribed non-uniform correlation structure, *Opt Lett*, 45(2020)3824–3827.
17. Hyde M W IV, Synthesizing general electromagnetic partially coherent sources from random, correlated complex screens, *Optics*, 1(2020)97–113.
18. Tong R, Dong Z, Chen Y, Wang F, Cai Y, Setälä T, Fast calculation of tightly focused random electromagnetic beams: controlling the focal field by spatial coherence, *Opt Express*, 28(2020)9713–9727.
19. Zhu X, Yu J, Wang F, Chen Y, Cai Y, Korotkova O, Synthesis of vector nonuniformly correlated light beams by a single digital mirror device, *Opt Lett*, 46(2021)2996–2999.
20. Martínez-Herrero R, Piquero G, Santarsiero M, Gori F, González de Sande J C, A class of vectorial pseudo-Schell model sources with structured coherence and polarization, *Opt Laser Technol*, 152(2022)108079; doi.org/10.1016/j.optlastec.2022.108079.
21. Miller W, *Symmetry and Separation of Variables*, (Addison-Wesley), 1977.
22. Gori F, Korotkova O, Modal expansion for spherical homogeneous sources, *Opt Commun*, 282(2009)3859–3861.

23. Borghi R, Gori F, Korotkova O, Santarsiero M, Propagation of cross-spectral densities from spherical sources, *Opt Lett*, 37(2012)3183–3185.
24. Xu C, Abbas A, Wang L.-G, Zhu S.-Y, Zubairy M S, Wolf effect of partially coherent light fields in two-dimensional curved space, *Phys Rev A*, 97(2018)063827; doi.org/10.1103/PhysRevA.97.063827.
25. Xu C, Wang L.-G, Theory of light propagation in arbitrary two-dimensional curved space, *Photon Res*, 9(2021)2486–2493.
26. Shao Z, Wang Z, Propagation and transformation of a light beam on a curved surface, *Opt Express*, 29(2021)8626–8634.
27. Schultheiss V H, Batz S, Peschel U, Light in curved two-dimensional space, *Advances in Physics: X*, 5(2020) 1759451; doi.10.1080/23746149.2020.1759451.
28. Agarwal G S, Gbur G, Wolf E, Coherence properties of sunlight, *Opt Lett*, 29(2004)459–461.
29. Divitt S, Novotny L, Spatial coherence of sunlight and its implications for light management in photovoltaics, *Optica*, 2(2015)95–103.
30. Petrov E Y, Kudrin A V, Exact axisymmetric solutions of the Maxwell equations in a nonlinear nondispersive medium, *Phys Rev Lett*, 104(2010)190404; doi.org/10.1103/PhysRevLett.104.190404.
31. Xiong H, Si L.-G, Huang P, Yang X, Analytic description of cylindrical electromagnetic wave propagation in an inhomogeneous nonlinear and nondispersive medium, *Phys Rev E*, 82(2010)057602; doi.org/10.1103/PhysRevE.82.057602.
32. Hyde M W, Bogle A E, Havrilla M J, Scattering of a partially-coherent wave from a material circular cylinder, *Opt Express*, 21(2013)32327–32339.
33. de Sande J C G, Korotkova O, Martínez-Herrero R, Santarsiero M, Piquero G, Failla A V, Gori F, Partially coherent spherical sources with spherical harmonic modes, *J Opt Soc Am A*, 39(2022)C21–C28.
34. Martínez-Herrero R, Korotkova O, Santarsiero M, Piquero G, deSande J C G, Failla A V, Gori F, Cylindrical partially coherent scalar sources, *Opt Lett*, 47(2022)5224–5227.
35. Santarsiero M, deSande J C G, Korotkova O, Martínez-Herrero R, Piquero G, Gori F, Three-dimensional polarization of fields radiated by partially coherent electromagnetic cylindrical sources, *Opt Lett*, 48(2023)2476–2479.
36. Santarsiero M, deSande J C G, Korotkova O, Martínez-Herrero R, Piquero G, Gori F, Partially Coherent Cylindrical Vector Sources, *Photonics*, 10(2023)831; doi. 10.3390/photonics10070831.
37. Setälä T, Tervo J, Friberg A T, Complete electromagnetic coherence in the space–frequency domain, *Opt Lett*, 29(2004)328–330.
38. Wolf E, Introduction to the Theory of Coherence and Polarization of Light, (Cambridge University Press), 2007.
39. Setälä T, Shevchenko A, Kaivola M, Friberg A T, Degree of polarization for optical nearfields, *Phys Rev E*, 66(2002)016615; doi.org/10.1103/PhysRevE.66.016615.
40. Ellis J, Dogariu A, Ponomarenko S, Wolf E, Degree of polarization of statistically stationary electromagnetic fields, *Opt Commun*, 248(2005)333–337.
41. Auñón J M, Nieto-Vesperinas M, On two definitions of the three-dimensional degree of polarization in the near field of statistically homogeneous partially coherent sources, *Opt Lett*, 38(2013)58–60.
42. Luis A, Degree of polarization for three-dimensional fields as a distance between correlation matrices, *Opt Commun*, 253(2005)10–14.
43. Gil J J, Ossikovski R, Polarized Light and the Mueller Matrix Approach, (Boca Raton: CRC Press, Taylor & Francis Group), 2016.
44. Tervo J, Setälä T, Friberg A T, Degree of coherence for electromagnetic fields, *Opt Express*, 11(2003)1137–1143.
45. Korotkova O, Wolf E, Spectral degree of coherence of a random three-dimensional electromagnetic field, *J Opt Soc Am A*, 21(2004)2382–2385.
46. Gori F, Santarsiero M, Borghi R, Maximizing Young’s fringe visibility through reversible optical transformations, *Opt Lett*, 32(2007)588–590.
47. Martínez-Herrero R, Mejías P M, Maximum visibility under unitary transformations in two-pinhole interference for electromagnetic fields, *Opt Lett*, 32(2007)1471–1473.
48. Luis A, Degree of coherence for vectorial electromagnetic fields as the distance between correlation matrices, *J Opt Soc Am A*, 24(2007)1063–1068.

49. Martínez-Herrero R, Mejías P M, Piquero G, Characterization of partially polarized light fields, (Springer Series in Optical Science, Springer), 2009.
50. Gbur G J, Mathematical Methods for Optical Physics and Engineering, (New York: Cambridge University Press), 2011.
51. Arfken G B, Weber H J, Mathematical Methods for Physicists, (New York: Elsevier, Academic Press), 6th edn, 2005.
52. Papas C H, Theory of Electromagnetic Wave Propagation, (New York: Dover), 2003.
53. Panofsky WKH, Philips M, Classical Electricity and Magnetism, (New York: Dover), 2005.
54. Gori F, Santarsiero M, Simon R, Piquero G, Borghi R, Guattar G, Coherent-mode decomposition of partially polarized, partially coherent sources, *J Opt Soc Am A*, 20(2003)78–84.
55. Tervo J, Setälä T, Friberg A T, Theory of partially coherent electromagnetic fields in the space–frequency domain, *J Opt Soc Am A*, 21(2004)2205–2215.

[Received: 25.11.2023; accepted: 15.03.2024]



Juan C Gonzalez de Sande obtained his degree in Physics from the Universidad Autónoma de Madrid in 1987, and his Ph D degree from the Universidad Complutense de Madrid in 1994 and since 2017 he is Professor at the Universidad Politécnica de Madrid. He has worked on the optical characterization of technological materials (ellipsometry, polarimetry) and on the generation, analysis and application of non-uniformly polarized beams and partially coherent beams. e mail: juancarlos.gonzalez@upm.es



Rosario Martínez-Herrero is Full Professor at Complutense University of Madrid (UCM), where she teaches Optics. She served as Topical Editor of Optics Letters and of Journal of the Optical Society of America A. She is a Fellow of Optica. RMH performed research activity on several topics in optics focusing his attention on characterization and propagation of partially polarized and partially coherent beams and highly focused fields. e mail: rosarmar@ucm.es



Gemma Piquero is Full Professor in Physics at the Optics Department in the Faculty of Physics of the Complutense University of Madrid (UCM) in Spain. She received her Ph D degree in Physics from UCM in 1994. Currently her interest is focused on the spatial and vectorial characterization and synthesis of light beams, both from the theoretical and experimental point of view. The aspects considered are, among others, beam shaping, coherence, polarization, full Poincaré polarimetry and parameterization, characterization and shaping of optical beams.

e mail: piquero@ucm.es



Olga Korotkova is a Professor of Physics and the Associate Chair of the Physics Department, at the University of Miami, Florida, USA. Her specialty for the last 20 years was classical statistical optics. She is the author of two monographs in this field and the author/co-author of over 250 peer-reviewed papers. She is also the Fellow of the Optical Society of America and currently serves as the Editor-in-Chief the Journal of Optical Society of America A.

e mail: o.korotkova@miami.edu



Massimo Santarsiero is Full Professor of Physics at “Roma Tre” University, where he teaches General Physics, Optics, and Photonics. His scientific interests mainly concern study and characterization of partially coherent sources and beams, propagation and diffraction of coherent electromagnetic fields, polarimetry. He is Senior Member of Optica and Colaborador Honorífico of the Complutense University of Madrid. During his career, he has been the Italian Representative at International Commission for Optics and member of the editorial boards of Journal of Optics A, Optics Express, and Photonics. e mail: msantarsiero@uniroma3.it



Franco Gori is Professor emeritus at the University “Roma Tre”. He taught Physics, Optics, Quantum Electronics, and other courses for engineers and physicists. He is a member of the Advisory Board of Optics Communications. He served as Topical Editor and Editor in Chief of Journal of the Optical Society of America A. He is a Fellow of Optica and of the European Optical Society. F. Gori performed research activity, both theoretically and experimentally, on several topics in optics focusing his attention on coherence theory, optical processing, light field propagation, inverse problems. e mail: franco.gori@uniroma3.it